

Photophysics of all-*trans*-retinoic acid (ATRA) chemisorbed to nanoparticulate TiO₂: evidence for TiO₂* to ATRA energy transfer and reverse electron transfer sensitisation

M.R.V. Sahyun^{a,*}, N. Serpone^b

^a Department of Chemistry, University of Wisconsin, Eau Claire, WI 54702, USA

^b Department of Chemistry and Biochemistry, Concordia University, 1455, boul. de Maisonneuve, O., Montréal, Québec, Canada H3G 1M8

Received 24 December 1997; accepted 20 January 1998

Abstract

The photophysics of all-*trans*-retinoic acid (ATRA) in methanol solution and of the system comprising ATRA chemisorbed to nanoparticulate TiO₂ have been examined in methanol solution and in aqueous dispersion (pH = 7), respectively. We found evidence for two closely spaced singlet excited states of ATRA, tentatively assigned as $n-\pi^*$ and $\pi-\pi^*$, with the former primarily responsible for ATRA fluorescence. The lifetime for this $^1(n-\pi^*)$ state in methanol solution is (55 ± 3) ps. The principal decay pathway of ATRA observable by picosecond transient absorption spectroscopy is photoionization. Under our conditions, photoionization is monophotonic and proceeds directly from the S₁ state of ATRA, yielding the corresponding radical cation, ATRA^{•+}. Electrochemical characterization of ATRA by square wave voltammetry supports this interpretation. ATRA chemisorbs to TiO₂ at pH 7 in large part by deprotonation, i.e., it is present on the anatase surface as the conjugate anion of ATRA. This species is much more fluorescent than free ATRA in solution. On laser flash photolysis at 355 nm, the principal observable photoproduct was deep trapped electrons in TiO₂. Unlike the TiO₂ preparation without ATRA, these species appear only slowly after photoexcitation. A mechanism is proposed, whereby chemisorbed ATRA quenches the initially photoexcited TiO₂ by energy transfer, followed by rate-limiting injection of electrons into the conduction band of TiO₂. The photoholes remain trapped in the ATRA. © 1998 Elsevier Science S.A. All rights reserved.

Keywords: Photophysics; All-*trans*-retinoic acid; Nanoparticulate TiO₂

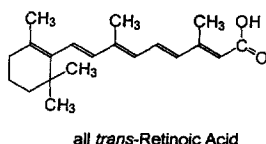
1. Introduction

We have recently initiated systematic studies of the photophysics of retinoid chromophores chemisorbed to nanoparticulate TiO₂. The rationale for this work is twofold: (1) such systems may serve as models of the visual photoreceptor, insofar as we anticipate that photoisomerization of the retinoid chromophore may be coupled to a photoelectronic response, in this case electron transfer between the chromophore and the semiconductive particle; (2) from the point of view of photocatalysis, electron transfer between the chemisorbed chromophores and the semiconductive TiO₂ particles can be envisioned as creating a system of nanoparticles coated with an array of 'molecular wires' which may, in turn, serve to interconnect the photocatalyst (TiO₂) with an external chemical system.

With regard to the first possibility, we further envision that an ensemble of such retinoid-sensitized nanoparticles incorporated in a composite membrane may comprise a synthetic image receptor, as has already been demonstrated for thin films of bacteriorhodopsin [1,2]. Vectorial, image-wise illumination of such a device should produce a photovoltage by operation of the Demmer effect [3–5]. The resulting image-wise, intensity-modulated charge pattern could be read out by external electronics for digital image capture applications.

For these preliminary studies, we chose to use as the chromophore all-*trans*-retinoic acid (ATRA), anticipating its efficient chemisorption to anatase or rutile surfaces by reaction of the carboxylic acid functionality. ATRA is commercially available, and the efficiency of spectral sensitisation of TiO₂ using dyes that chemisorb in this manner is well known [6]. By way of experimental protocol, we took the study of spectral sensitisation of TiO₂ nanoparticles reported by Arbour et al. [7] as a model.

* Corresponding author.



2. Experimental

2.1. Materials

The nominally all-*trans*-retinoic acid was obtained from Aldrich Chemical and used without further purification. Methanol was HPLC grade from BDH Chemicals. An anatase titania nanosol was prepared according to the method of Moser [8], which as obtained comprised $25 \text{ g l}^{-1} \text{ TiO}_2$ in water at pH 2. Expected average particle diameter in such a preparation is 120–130 Å. To enable chemisorption of ATRA, the aquosol was diluted to 1 g/l with 0.01 M, pH 7 phosphate buffer in the presence of 1 wt.% polyvinylalcohol (Hoechst Mowiol 98–10). The resulting dispersion was ultrasonicated 10 min to overcome tendency of the TiO_2 to flocculate under these conditions. A clear, stable, neutral aquosol resulted. The ATRA was chemisorbed onto the TiO_2 by introduction of 0.1 ml of a $2.0 \times 10^{-3} \text{ M}$ solution of ATRA in methanol into 10 ml of the pH 7 dispersion.

2.2. Methods

Absorption spectra were recorded on a Shimadzu UV-265 double beam spectrophotometer. Fluorescence spectra were recorded on a Perkin-Elmer MPF-44B fluorescence spectrophotometer, operating in the ratio mode. Spectra are otherwise uncorrected.

Laser flash spectroscopy was carried out under otherwise similar conditions to those used earlier [7]. The frequency-tripled output of a Nd:YAG laser was used to excite the solution samples in a 2-mm quartz cell at 355 nm, with a pulse width of ca. 30 ps (full width at half-maximum, FWHM). Unless otherwise specified, pulse energies were $(2.5 \pm 0.4) \text{ mJ/pulse}$. Instrumentation for pulse generation, selection and delay, and for recording and analysis of the transient absorption spectra has been described previously [9,10]. Fluorescence rise and decay profiles were recorded on a Hamamatsu streak camera [11,12], with 2.2 ps/channel resolution.

Electrochemical analyses were carried out on a Bioanalytical Systems CV50 voltammetric analyzer with a Pt working electrode and an Ag–AgCl reference electrode. For electrochemical characterization, ATRA was made up 0.001 M in a 90:10 acetonitrile–methanol solvent system incorporating 0.01 M tetrabutyl–ammonium tetrafluoroborate (Aldrich) supporting electrolyte. Owing to possible irreversible electrochemistry of ATRA, e.g., deprotonation concerted

with one-electron oxidation, square wave voltammetry with 25 mV pulse height and 5 mV steps was employed [13,14]. The voltammetric analysis was calibrated using ferrocene in the same solvent–electrolyte system.

3. Results and discussion

3.1. Absorption spectroscopy

The optical bandgap of the TiO_2 preparation at pH 2 is reportedly 3.44 eV [8]. The absorption spectrum obtained for the nanosol after adjustment to pH 7 allowed estimation [15] of a bandgap, $E_{\text{bg}} = (3.29 \pm 0.04) \text{ eV}$, that is representative of anatase titania. The red shift in the band edge is probably due to relaxation of lattice contraction in the particles of the starting nanosol [8].

The absorption spectrum of ATRA in methanol exhibited λ_{max} at 348 nm ($\epsilon = 6.8 \times 10^4 \text{ M}^{-1} \text{ cm}^{-1}$) with a secondary shoulder at ca. 375 nm (Fig. 1a). The absorption peak in methanol is slightly blue-shifted from the value of 357 nm observed by Motto et al. [16] for chromatographically pure ATRA in a complex, mixed solvent system, but close to the value of 350 nm reported by Takashima et al. [17] for ATRA

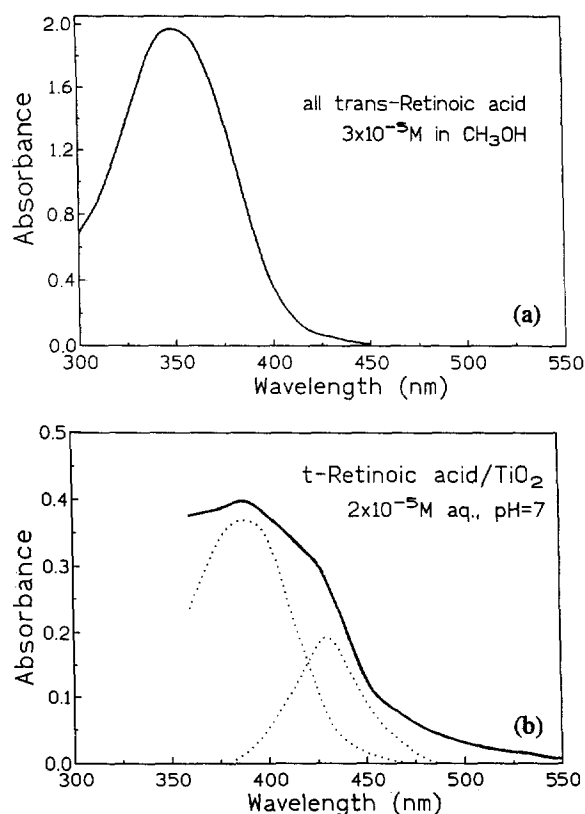


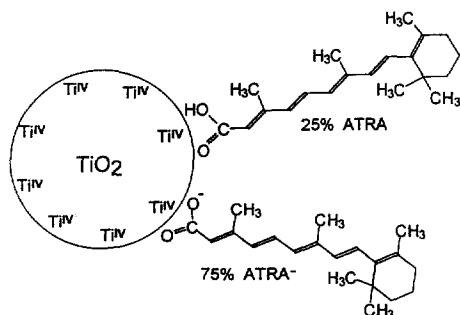
Fig. 1. (a) Absorption spectrum of ATRA, $3 \times 10^{-5} \text{ M}$ in methanol; (b) absorption spectrum of ATRA, $2 \times 10^{-5} \text{ M}$ chemisorbed onto nanoparticulate TiO_2 at pH 7 (aq.). Dotted lines indicate possible deconvolution of the absorption envelope for the chemisorbate into components assigned to ATRA and its conjugate base.

in absolute ethanol. The 375 nm shoulder does not correspond to any of the products, principally retinoic acid geometric isomers, which might result on adventitious degradation of initially pure ATRA [16,17].

By analogy to all-*trans*-retinal, where well-defined spectral assignments have been made [28], we assign the highly allowed electronic transition corresponding to λ_{\max} to the lowest lying $^1(\pi-\pi^*)$ excitation of the polyene chain. The long wavelength shoulder (S_1 for ATRA) may accordingly be an $n-\pi^*$ transition involving the lone pair electrons of the carboxyl group. It is obvious that the absorption envelope of Fig. 1a comprises at least two electronic transitions, as unit transition probability, $f=1$, would limit the FWHM bandwidth of a single absorption of the observed extinction coefficient to ca. 3675 cm^{-1} , while the observed FWHM bandwidth is 5770 cm^{-1} .

The absorption spectrum for ATRA chemisorbed on TiO_2 was obtained as the difference spectrum between spectra recorded for dyed ($2 \times 10^{-5}\text{ M}$ ATRA) and undyed TiO_2 nanosols at 1 g l^{-1} concentration (Fig. 1b). This spectrum exhibits a strongly red-shifted λ_{\max} at 387 nm, with a long-wavelength shoulder at ca. 420 nm. The red shift on adsorption of the chromophore to a high dielectric constant substrate is expected [19]. By comparison, a solution of methanolic ATRA diluted with the pH 7 aqueous buffer exhibits, in addition to the principal absorption of ATRA observable in methanol, a new band at 420 nm which we assign to the conjugate anion of ATRA. We therefore infer that ATRA adsorbs to TiO_2 in part, but not completely, through deprotonation, i.e., by acid-base reaction with the TiO_2 surface OH^- groups, and that both ATRA and its conjugate base are present on the TiO_2 surface. The conjugate anion is presumably present as a Ti^{IV} salt.

The spectrum was deconvoluted as shown in the figure with the assumptions that all the ATRA in the system is accounted for by the absorption in the accessible spectral window; and that the electronic transition centered on 387 nm has the same extinction coefficient as free ATRA in solution; also unit transition probability. We accordingly infer that adsorbed, but not deprotonated, ATRA represents ca. 25% of the total ATRA present in the system, and, thus, up to 75% of the adsorbed ATRA may be present in the chemisorbed conjugate anion form.



3.2. Fluorescence spectroscopy

The steady-state fluorescence emission and excitation spectrum of ATRA was recorded for the compound $2 \times 10^{-6}\text{ M}$ in methanol and illustrated in Fig. 2 (dashed curves). The wavelength of maximum emission to be 470 nm, with a secondary maximum in the spectrum at ca. 505 nm. In the excitation spectrum the maximum emissive response was observed at 382 nm, corresponding to the long wavelength shoulder in the absorption spectrum. A shoulder was observed in the excitation spectrum at 345 nm, corresponding to λ_{\max} for absorption. We infer that the state (S_1) responsible for the long wavelength shoulder is primarily emissive, and that the slightly higher lying state (S_2) which corresponds to the absorption maximum can access other deactivation pathways, e.g., isomerization (see below) in competition with internal conversion to S_1 . This interpretation is consistent with the tentative assignment of S_2 as the lowest lying $\pi-\pi^*$ transition of the polyene chain and S_1 as an $n-\pi^*$ transition (see Scheme 1). The large Stokes shift for ATRA (4900 cm^{-1}) suggests, nevertheless, a substantial torsional relaxation of the polyene chain prior to fluorescence from S_1 .

The fluorescence intensified by approximately one order of magnitude when the *trans*-retinoic acid was adsorbed to TiO_2 . Emission and excitation spectra recorded for ATRA under these conditions are also shown in Fig. 2 (solid curves). Surprisingly, the λ_{\max} for emission was blue shifted to 425 nm, compared to that for dissolved ATRA, with a secondary emission maximum at 470 nm, corresponding to the emission by free ATRA. The excitation spectrum peaked at 412 nm corresponding to the absorption shoulder assigned above to the conjugate anion of ATRA on the TiO_2 surface. There is no inflection in the excitation spectrum at the wavelength of the absorption maximum. We infer that the emission of ATRA on TiO_2 is dominated by that of the conjugate anion, and that it is much less prone to radiationless relaxation than is the free acid in solution. Interestingly, the 0–0 energies of

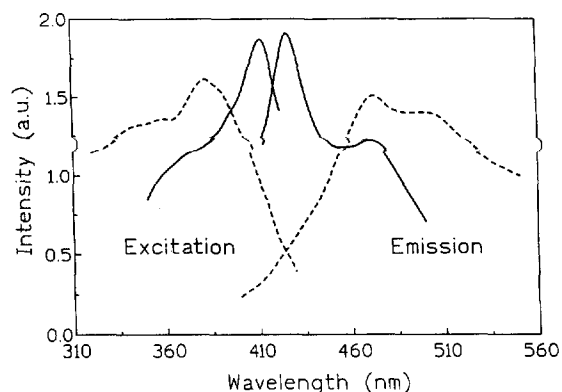


Fig. 2. Fluorescence emission and excitation spectra for ATRA. Dashed curves: free ATRA in methanol; excitation spectrum recorded with emission monitored at 470 nm; emission spectrum recorded for excitation at 375 nm. Solid curves: ATRA chemisorbed on nanoparticulate TiO_2 at pH 7 (aq.); excitation spectrum recorded with emission monitored at 425 nm; emission spectrum recorded with excitation at 410 nm.

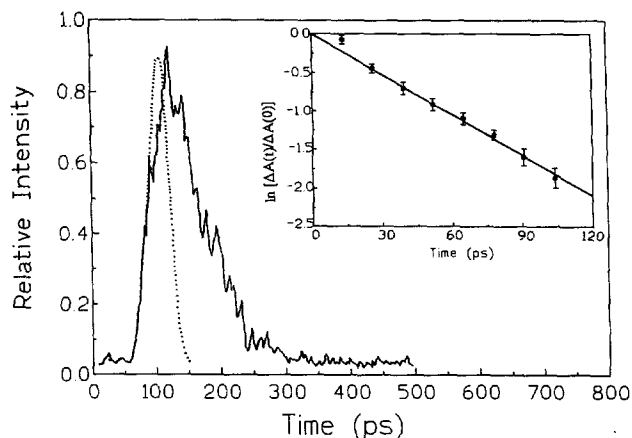


Fig. 3. Picosecond-resolved rise and decay of ATRA fluorescence in methanol solution with laser pulse excitation at 355 nm. Streak camera profile: dashed trace illustrates exciting laser pulse width (30 ps, FWHM). Inset: exponential analysis of fluorescence decay after the end of the laser pulse.

the emissive states of ATRA in methanol solution and chemisorbed on TiO_2 are estimated to be about the same, 3.00 and 2.96 eV, respectively.

Radiationless deactivation of singlet excited ATRA involves isomerization about one or more of the conjugated double bonds of the retinoic chromophore [16,20], intersystem crossing (by analogy to other retinoid chromophores [21,22]), as well as photochemical reaction involving electron and/or hydrogen atom abstraction [23]. If the potential energy surface for isomerization from a $\pi\text{-}\pi^*$ singlet state resembles that proposed for cyanine dyes [24–27], it is likely that the isomerization and intersystem crossing processes are coupled, with both processes gated by torsional relaxation about C–C bonds of the polyene chain. By analogy to the same system [28,29], we would expect such torsional relaxation of ATRA to be significantly quenched when the mole-

cule is chemisorbed to a solid surface. The large enhancement of fluorescence quantum efficiency and dramatic reduction of the Stokes shift (to 740 cm^{-1}) when ATRA is chemisorbed to TiO_2 are thus not surprising.

3.3. Picosecond-resolved spectroscopy of ATRA

Appearance and decay of fluorescence of ATRA, $2 \times 10^{-6}\text{ M}$ in methanol, was followed by pulse laser excitation at 355 nm, coupled with streak camera detection [11,12]. A representative streak camera trace is shown in Fig. 3. Rise of fluorescence occurs within the laser pulse; decay was singly exponential with lifetime $\tau = (55 \pm 3)\text{ ps}$ ($r^2 = 0.996$), as shown in the inset of Fig. 3. Bondarev et al. [30] found $\tau = (80 \pm 8)\text{ ps}$ for ATRA in 90:10 hexane–ether solvent, in reasonable agreement with our estimate. From our estimate of τ and the natural radiative lifetime for ATRA, $\tau_{\text{nat}} = 1.7\text{ ns}$, calculated [31] from the parameters of the absorption spectrum, we estimate a fluorescence quantum efficiency, $\Phi_f = \tau/\tau_{\text{nat}}$, of ca. 0.035.

Direct pulse laser excitation of ATRA in methanol at 355 nm yields the transient absorption spectra illustrated in Fig. 4. During the laser pulse and at short delay times thereafter, a well-defined band centered on 450 nm is apparent, which can be identified with the S_1 state of ATRA [24–27]. It disappears within 200 ps consistent with the fluorescence lifetime measurement (see above). A second absorption band centered at ca. 595 nm appears in the interval up to 200 ps following excitation and is stable for up to 10 ns (limit of the experiment). Analysis of its growth according to pseudo-first order kinetics yields a rate constant $k = 0.014\text{ ps}^{-1}$, corresponding approximately to the reciprocal of the fluorescence lifetime, τ . We infer that this band is associated with a product of the radiationless decay of S_1 . It cannot be assigned to a geometrical isomer of ATRA [11,12], nor to the $T_1\text{-}T_n$ bands,

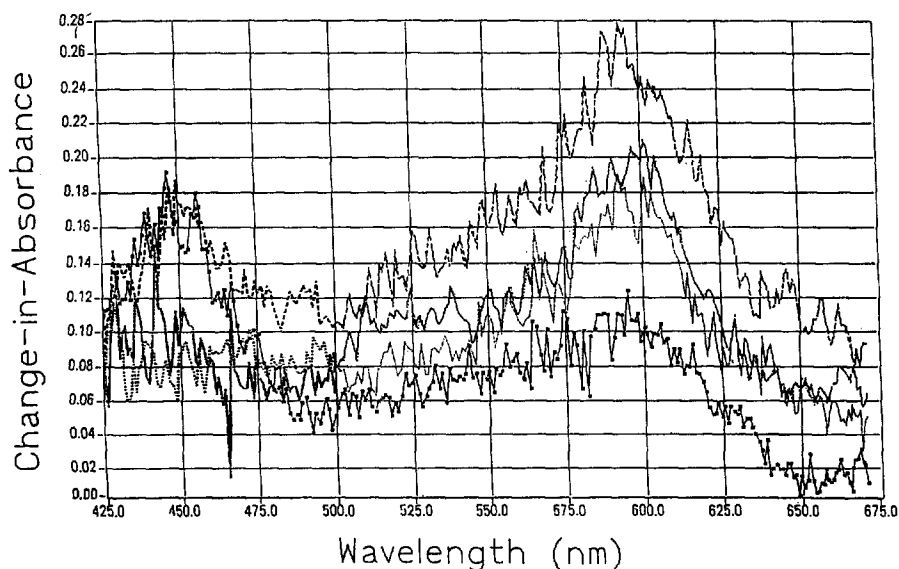


Fig. 4. Transient absorption spectra recorded (bottom-to-top at 600 nm) 20, 50, 100, and 200 ps, respectively, after laser pulse excitation of ATRA in methanol solution.

as the intersystem crossing products of retinoid chromophores are also usually observed at shorter wavelengths [22,32]. This absorption band does, however, occur in the same spectral regime as typical retinoid radical cations, including that derived from ATRA [33,34]. Monophotonic ionization of retinoid chromophores other than ATRA, e.g., retinol, is well known, but the photoionization of ATRA in methanol has been reported to be biphotonic [33]. We accordingly assign the 595 nm transient to the radical cation of ATRA.

The proposal of biphotonic photoionization is apparently inconsistent with our inference that the radical cation forms directly from S_1 ATRA. We therefore monitored the magnitude of the 595 nm transient 2 ns after pulse laser photolysis at 355 nm at varying laser pulse energies. These data are depicted in Fig. 5. The relationship between change-in-absorbance, ΔA , and pulse energy (mJ per pulse) is linear in the regime up to 2 mJ per pulse ($r^2 = 0.998$). Under our conditions, photoionization of ATRA is thus monophotonic. Monophotonic photoionization of retinyl acetate in methanol has been associated with the presence of water in the solvent [33]; our results may differ from those in the literature for ATRA for this reason. Formation of radical cation in this manner supports the hypothesis of Dillon et al. [23], namely that formation of radical products on photolysis of retinoid chromophores results from electron transfer to solvent.

3.4. Electrochemistry of ATRA

Square-wave voltammetry of ATRA yielded voltammograms peaking at (0.56 ± 0.03) and (0.50 ± 0.03) V vs. Ag–AgCl for the forward and reverse sweeps, respectively. Curve shapes corresponded to those calculated for reversible electron transfer [13]. We deduce that ATRA undergoes a reversible one-electron oxidation at +0.53 V vs. Ag–AgCl. By comparison, Park [35] has reported one-electron potentials of +0.74 V for β -carotene and +1.20 V for retinal, both vs. SCE. Subtraction of the 0–0 excitation energy for ATRA, as estimated above, from the observed potential, locates the HOMO level of the excited S_1 state ATRA (or, that is, the LUMO of ground state ATRA) at ca. –2.5 V (vs. Ag–AgCl), consistent with the feasibility of monophotonic photoionization of ATRA in solution.

3.5. Picosecond-resolved spectroscopy of the ATRA–TiO₂ system

When the streak camera experiment was carried out on ATRA in the presence of the nanoparticulate TiO₂, the results were indistinguishable from those presented for ATRA in Fig. 3; however, the signal intensity was about threefold weaker. We presume that fluorescence from this system excited at 355 nm arises primarily from a small amount of free ATRA which must be present in the system (see above), and not from the chemisorbed conjugate anion, whose absorption lies ca. 60 nm to the red of the pump wavelength.

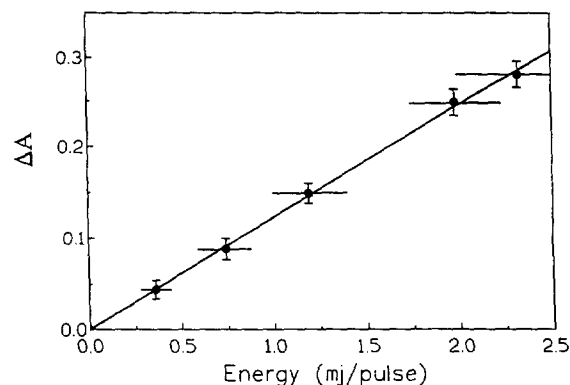


Fig. 5. Laser pulse energy (mJ per pulse) dependence of change-in-absorbance (ΔA) at 590 nm observed 2 ns after laser flash photolysis of ATRA in methanol.

The chemisorbed dye does not absorb the pump laser pulse in our system, unlike the sensitizing dyes on TiO₂ studied by Arbour et al. [7].

Excitation of an aqueous suspension of TiO₂ (pH=7) alone under the conditions of laser flash photolysis probed by transient absorption spectroscopy yielded a weak ($\Delta A = \text{ca. } 0.05$) light absorbing transient within the pulse (< 30 ps) as previously reported [9]. This transient decays rapidly and is barely detectable after 200 ps. It was thus not expected to interfere with detection of transient intermediates associated with ATRA.

Laser flash photolysis at 355 nm of the TiO₂ suspension with chemisorbed ATRA led to the transient absorption spectra shown in Fig. 6. Under these conditions most of the exciting radiation at 355 nm is, however, absorbed by the TiO₂ nanoparticles, which exhibit an optical density of ca. 0.4 at this wavelength in the 2 mm cell. The distribution of transient absorption is typical of that observed on photoexcitation of nanoparticulate TiO₂ [9] and usually assigned to photoelectrons localized in traps representing a distribution of trap depths [9,15]. The salient feature of the data of Fig. 6 is that trapped photoelectrons form in TiO₂ on a time scale entirely different from that for direct irradiation of the nanosol in the absence of ATRA, even though most of the actinic radiation is absorbed by TiO₂.

One mechanism which can rationalize these results can be described thus (Scheme 2): (i) photoexcitation (step 1) in TiO₂ is quenched by efficient energy transfer from TiO₂* to chemisorbed ATRA (step 2), in competition with radiative and non-radiative electron-hole recombination (step 3), leading to formation of the S_1 state of the adsorbate (step 4); (ii) subsequently, the excited adsorbate then transfers an electron to the conduction band of TiO₂ (step 5) on the time scale of the experiment in competition with other photophysical and photochemical processes (step 7); photoholes accordingly remain trapped on the ATRA molecules for times much longer than 10 ns, our time window limit.

The first mechanistic postulate (i) is thermodynamically feasible as the 0–0 energy of S_1 chemisorbed ATRA is esti-

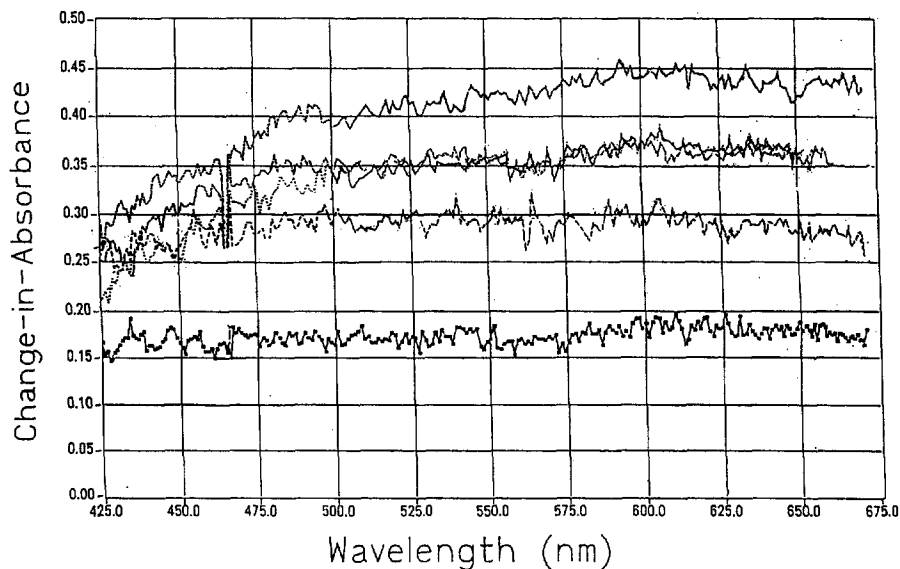


Fig. 6. Transient absorption spectra recorded for laser flash excitation of the TiO_2 nanosol at pH 7 with chemisorbed ATRA. Delay times in this experiment correspond (bottom-to-top) to 1, 2, 3.5, 5 and 10 ns after laser pulse excitation.

mated to be 2.96 eV (see above). The optical band gap of the TiO_2 used in these experiments is 3.44 eV [8].

The description of energy transfer from a localized state near the surface of a TiO_2 particle to an adsorbate is symmetrical with the description of energy transfer from an excited adsorbate to localized states in semiconductor. The theory of the latter is well developed [36–38]. Accordingly, efficient dipole–dipole energy transfer requires resonance between the donor and acceptor states. Luminescence spectroscopy of these TiO_2 colloids evidences emissive states at 3.05 and 2.91 eV (vs. 2.97 eV for the 0–0 band of ATRA and 2.77 eV for the chemisorbed conjugate anion) which have been assigned as the indirect $X_{2b} \rightarrow \Gamma_{1b}$ and $X_{1a} \rightarrow \Gamma_{1b}$ transitions of TiO_2 , respectively [15]. Furthermore, energy transfer may be kinetically preferable to hole transfer at the TiO_2 interface owing to the large mismatch between the energy levels of the TiO_2 valence band and the HOMO of ATRA, as estimated electrochemically, above.

Kinetics of appearance of the absorption assigned to trapped photoelectrons were treated as pseudo-first order, leading to a rate constant of 0.42 ns^{-1} ($r^2 = 0.996$). According to the proposed mechanism, the reciprocal of this rate constant, $\tau = 2.5 \text{ ns}$, defines the lifetime of the emissive S_1 state of the chemisorbed ATRA. This value is consistent with the observed high efficiency for fluorescence from ATRA present as the conjugate anion chemisorbed to TiO_2 . By the method of Strickler and Berg [31], we estimate the natural radiative lifetime for ATRA conjugate anion adsorbed to titania as 2.0 ns.

An alternative mechanism presupposes that photoholes, generated on laser pulse excitation of TiO_2 , are transferred rapidly to the chemisorbed ATRA, thus effectively eliminating electron-hole recombination. Accordingly, the measured rate constant for appearance of the light absorbing transient would correspond to rate-limiting deep trapping of photoe-

lectrons. This interpretation is inconsistent with the rapid appearance of the trapped electron absorption spectrum in the absence of ATRA, compared to its slow appearance in the presence of ATRA. It would also be surprising for ATRA to be a much more efficient hole trapping species than the polyvinylalcohol, which is already present in much higher concentration.

4. Conclusions

We have studied the photophysics of ATRA in methanol solution and of the system comprising ATRA chemisorbed to nanoparticulate TiO_2 . We found evidence for two closely spaced singlet excited states of ATRA itself, tentatively assigned as $n-\pi^*$ and $\pi-\pi^*$, with the former primarily responsible for ATRA fluorescence. The lifetime for this state in methanol solution was measured as ca. 55 ps. On laser flash photolysis of ATRA in methanol solution, the principal decay pathway observable by transient absorption spectroscopy was photoionization. Under our conditions, photoionization is monophotonic and proceeds directly from the S_1 state of ATRA, yielding the corresponding radical cation ATRA^+ . Electrochemical characterization of ATRA by square wave voltammetry supports this interpretation.

ATRA chemisorbs to TiO_2 at pH 7 in large part by deprotonation, i.e., it is present on the anatase surface as the conjugate anion of ATRA. This species is much more fluorescent than free ATRA in solution. On laser flash photolysis, the principal observable photoproduct was deep trapped electrons in TiO_2 . Unlike the case of the TiO_2 preparation without ATRA, these species appear only slowly after photoexcitation. We propose a mechanism whereby chemisorbed ATRA quenches the initially photoexcited TiO_2 by energy transfer, followed by rate-limiting injection of electrons from the

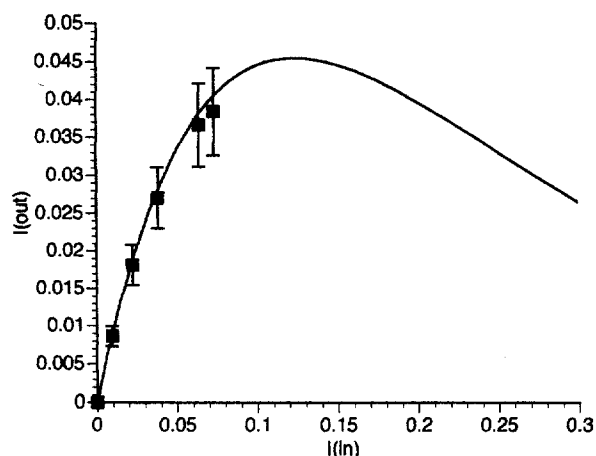


Fig. 7. Plot of Eq. (A2) illustrating hypothetical optical limiting behavior of the retinoic acid-nanoparticulate TiO_2 system (see Appendix A); input and output fluences in J cm^{-2} .

resulting excited ATRA into the conduction band of TiO_2 . The photoholes remain trapped in the ATRA.

In summary, we have demonstrated that TiO_2 nanoparticles with chemisorbed ATRA represent a system in which efficient electron-hole separation may be achieved on photoexcitation, with long-term stability (> 10 ns) of the charge separated state. Given the intense broad spectral absorption of the trapped photoelectrons, this system may be useful in optical limiting applications [39] (see Appendix A), as well as in the proposed areas of image sensing and as a model for visual response.

Acknowledgements

Support of this work by the Natural Sciences and Engineering Research Council of Canada (in Montréal) and by the State of Wisconsin (Eau Claire) is gratefully acknowledged. We thank Dr. Jacques Moser of the Ecole Polytechnique Fédérale of Lausanne, Switzerland, for a gift of the TiO_2 preparation, and Ms. Monica Chadha (Eau Claire) and Mr. Reza Danesh (Montréal) for their able technical assistance. Instrumentation at Eau Claire was provided by a gift from 3M, St. Paul.

Appendix A

The ATRA-nanoparticulate titania system described in this paper is an example of a photochromic system. Its response to incident ultra-band gap laser radiation has been shown to be monophotonic, and the absorption change, ΔA , accordingly varies with incident intensity, I_{in} , as

$$d\Delta A/dI_{\text{in}} = b\Phi\varepsilon \quad (\text{A1})$$

where b is the fraction of the incident laser radiation absorbed by the nanoparticulate material, Φ is the quantum yield for

formation of color centers in TiO_2 , and ε is the extinction coefficient of the formed centers. Introduction of the molar extinction coefficient implies that light absorption by these centers obeys Beer's Law. Accordingly, the laser intensity, I_{out} , transmitted by a sample of the system on continued irradiation after formation of the color centers is given by

$$I_{\text{out}} = I_{\text{in}} \exp(-2.303 b\Phi\varepsilon I_{\text{in}}) \quad (\text{A2})$$

so that

$$dI_{\text{out}}/dI_{\text{in}} = I_{\text{in}} [-2.303 b\Phi\varepsilon \exp(-2.303 b\Phi\varepsilon I_{\text{in}})] + \exp(-2.303 b\Phi\varepsilon I_{\text{in}}) \quad (\text{A3})$$

Defining $I_0 = I_{\text{in}}$ for the case $dI_{\text{out}}/dI_{\text{in}} = 0$, we obtain

$$I_0 = (2.303 b\Phi\varepsilon)^{-1} \quad (\text{A4})$$

Eq. (A4) defines the condition of optical bistability: for $I_{\text{in}} < I_0$, I_{out} increases monotonically with I_{in} , while for $I_{\text{in}} > I_0$, I_{out} decreases with increasing I_{in} . Thus, systems which obey the conditions described by Eq. (A1) and A2 are optical limiters with switching threshold I_0 .

From the slope of Fig. 5 (corresponding to Eq. (A1)) with ΔA measured 2 ns after laser flash irradiation, and the geometry of the experiment, we obtain $b\Phi\varepsilon = (3.5 \pm 0.3) (\text{J cm}^{-2})^{-1}$. Accordingly, Eq. (A4) predicts $I_0 = (0.12 \pm 0.01) \text{J cm}^{-2}$, comparable to the switching thresholds of other optical limiting systems which have recently been proposed for practical application [39–46], for which I_0 ranges from 0.025 – 5J cm^{-2} . Unfortunately, this I_0 estimate lay outside the regime of our experimental capabilities ($I_{\text{in}} < 0.1 \text{J cm}^{-2}$), and as a result was not experimentally verifiable. Fig. 7 shows a plot of Eq. (A2) using the experimentally derived estimate for $b\Phi\varepsilon$.

References

- [1] T. Miyasaka, K. Koyama, I. Itoh, *Science* 255 (1992) 342.
- [2] B. Robertson, E.P. Lukashov, *Biophys. J.* 68 (1995) 1507.
- [3] H. Dember, *Phys. Z.* 32 (1931) 554, 806.
- [4] H. Dember, *Phys. Z.* 33 (1932) 207.
- [5] V.G. Vlasov, P.V. Meikljar, *Photogr. Sci. Eng.* 17 (1973) 343.
- [6] J. Moser, S. Punchihewa, P.P. Infelta, M. Grätzel, *Langmuir* 7 (1991) 3012.
- [7] C. Arbour, D.K. Sharma, C.H. Langford, *J. Phys. Chem.* 94 (1991) 331.
- [8] J. Moser, PhD Dissertation, Thesis No. 616, Ecole Polytechnique Fédérale de Lausanne, Lausanne, Switzerland, 1986.
- [9] G. Rothenberger, J. Moser, M. Grätzel, N. Serpone, D.K. Sharma, *J. Am. Chem. Soc.* 107 (1985) 8054.
- [10] N. Serpone, M.A. Jamieson, D.K. Sharma, R. Danesh, J. Ramsden, M. Grätzel, *Chem. Phys. Lett.* 115 (1985) 473.
- [11] W. Yu, in: C.V. Shank, E.P. Ippen, S.L. Shapiro (Eds.), *Picosecond Phenomena*, Springer, Berlin, 1978, pp. 346ff.
- [12] K.L. Sala, R.W. Yip, R. LeSage, *Appl. Spectrosc.* 37 (1983) 273.
- [13] P.T. Kissinger, W.R. Heineman, *Laboratory Techniques in Electroanalytical Chemistry*, Chap. 5, Marcel Dekker, New York, 1984.
- [14] R. Samuelsson, J.J. O'Dea, J. Osteryoung, *Anal. Chem.* 52 (1980) 2215.
- [15] N. Serpone, D. Lawless, R.F. Khairutdinov, E. Pellizzetti, *J. Phys. Chem.* 99 (1995) 16655.

- [16] M.G. Motto, K.L. Facchine, P.F. Hamburg, D.J. Burinsky, R. Dunphy, A.R. Oyler, M.L. Cotter, *J. Chromatogr.* 481 (1989) 255.
- [17] Y. Takashima, T. Nakajima, M. Washitake, T. Anmo, M. Sugiura, H. Matsumaru, *Chem. Pharm. Bull.* 27 (1979) 12.
- [18] G. Drikos, G. Rueppel, *Photochem. Photobiol.* 40 (1984) 93.
- [19] W. West, B.H. Carroll, in: T.H. James (Ed.), *Theory of the Photographic Process*, 3rd edn., Macmillan, New York, 1966, p. 246ff.
- [20] R.W. Curley Jr., J.W. Fowble, *Photochem. Photobiol.* 47 (1988) 831.
- [21] K. Bhattacharya, P.K. Das, *Chem. Phys. Lett.* 116 (1985) 326.
- [22] K. Bhattacharya, S. Rajadurai, P.K. Das, *Tetrahedron* 43 (1987) 1701.
- [23] J. Dillon, E.R. Gaillard, P. Bilski, C.F. Chignell, K.J. Reszka, *Photochem. Photobiol.* 63 (1996) 680.
- [24] S.H. Ehrlich, *J. Phys. Chem.* 79 (1975) 2228, 2234.
- [25] F. Momicchioli, I. Baraldi, G. Berthier, *Chem. Phys.* 123 (1988) 103.
- [26] G. Ponterini, F. Momicchioli, *Chem. Phys.* 151 (1991) 111.
- [27] G. Ponterini, M. Caselli, *Ber. Bunsenges. Phys. Chem.* 96 (1992) 564.
- [28] D. Fassler, M. Baezold, *J. Photochem. Photobiol. A Chem.* 64 (1992) 359.
- [29] D. Fassler, M. Baezold, D. Baezold, *J. Mol. Struct.* 174 (1988) 383.
- [30] S.L. Bondarev, S.A. Tikhomirov, S.M. Bachilo, *Proc. SPIE* 1403 (1990) 497.
- [31] S.J. Strickler, R.A. Berg, *J. Chem. Phys.* 37 (1962) 814.
- [32] Z. Wang, W.G. McGimpsey, *J. Photochem. Photobiol. A Chem.* 93 (1996) 151 and references cited therein.
- [33] K.K.N. Lo, E.J. Land, T.G. Truscott, *Photochem. Photobiol.* 36 (1982) 139.
- [34] K. Bobrowski, R.K. Das, *J. Phys. Chem.* 89 (1985) 5079.
- [35] S.-M. Park, *J. Electrochem. Soc.* 125 (1978) 216.
- [36] R.R. Chance, A. Prock, R. Silbey, *Adv. Chem. Phys.* 37 (1978) 1.
- [37] A. Adams, R.W. Rendell, W.P. West, H.P. Broida, P.K. Hansma, H. Metiu, *Phys. Rev. B* 21 (1980) 5565.
- [38] P.M. Whitmore, H.J. Robota, C.B. Harris, *J. Chem. Phys.* 77 (1982) 1560.
- [39] H.M. Gibbs, *Optical Bistability—Controlling Light with Light*, Academic Press, New York, 1985.
- [40] S. Shi, W. Ji, S.H. Tang, J.P. Lang, X.Q. Xin, *J. Am. Chem. Soc.* 116 (1994) 3615.
- [41] J.W. Perry, K. Mansour, S.R. Marder, K.J. Perry, D. Alvarez Jr., I. Choong, *Opt. Lett.* 19 (1994) 625.
- [42] L.W. Tutt, N. Kost, *Nature* 356 (1992) 225.
- [43] F. Henari, J. Callaghan, H. Stiel, W. Blau, D.J. Cardin, *Chem. Phys. Lett.* 199 (1992) 144.
- [44] A. Kost, L.W. Tutt, M.B. Klein, T.K. Dougherty, W.E. Elias, *Opt. Lett.* 18 (1993) 224.
- [45] D.J. McLean, R.L. Sutherland, M.C. Brant, D.M. Brandelik, P.A. Fleitz, T. Pottenger, *Opt. Lett.* 18 (1993) 858.
- [46] M.R.V. Sahyun, S.E. Hill, N. Serpone, R. Danesh, D.K. Sharma, *J. Appl. Phys.* 79 (1996) 8030.